Exciton storage in CdSe/CdS tetrapod semiconductor nanocrystals: Electric field effects on exciton and multiexciton states

Su Liu,[1] Nicholas J. Borys,[1] Jing Huang,[2] Dmitri V. Talapin,[2] and John M. Lupton[1,3,*]

[1]*Department of Physics & Astronomy, University of Utah, 115 South 1400 East, Salt Lake City, Utah 84112, USA*
[2]*Department of Chemistry, The University of Chicago, 929 East 57th Street, GCIS E 205, Chicago, Illinois 60637, USA*
[3]*Institut für Experimentelle und Angewandte Physik, Universität Regensburg, Universitätsstrasse 31, 93053 Regensburg, Germany*

CdSe/CdS nanocrystal tetrapods are interesting building blocks for excitonic circuits, where the flow of excitation energy is gated by an external stimulus. The physical morphology of the nanoparticle, along with the electronic structure, which favors electron delocalization between the two semiconductors, suggests that all orientations of a particle relative to an external electric field will allow for excitons to be dissociated, stored, and released at a later time. While this approach, in principle, works, and fluorescence quenching of over 95% can be achieved electrically, we find that discrete trap states within the CdS are required to dissociate and store the exciton. These states are rapidly filled up with increasing excitation density, leading to a dramatic reduction in quenching efficiency. Charge separation is not instantaneous on the CdS excitonic antennae in which light absorption occurs, but arises from the relaxed exciton following hole localization in the core. Consequently, whereas strong electromodulation of the core exciton is observed, the core multiexciton and the CdS arm exciton are not affected by an external electric field.

I. INTRODUCTION

Semiconductor nanocrystals are frequently cited for their versatile optoelectronic properties,[1] yet surprisingly little is known about the excited states and their dynamics in the presence of an external electric field. In general, these states can be categorized as either quantum confined band states, or localized states, commonly referred to as traps, which are typically attributed to nanocrystal imperfections such as crystal defects and surface states. In particular, due to the large surface to volume ratio, nanoparticles are susceptible to the influence of surface defects, such as dangling bonds, which are capable of localizing charge.[2–6] Such charge localization can influence the electronic structure of the particle, to a first approximation, by the quantum-confined Stark effect,[6–9] and may also play a role in more subtle effects contributing to fluorescence intermittency.[5–7,10,11] One of the unresolved issues is the ways in which surface charge and surface traps in quantum dots relate to the underlying mechanism of blinking.[6,10,12,13] It has generally been assumed that blinking arises as a consequence of charging of the nanoparticle and an associated increase in the nonradiative Auger recombination rate.[10,14] The strong reduction of blinking in larger particles, most notably in vapor phase-grown self-assembled structures,[15] appears to support this conclusion, as does the sensitivity of fluorescence intermittency to surface modification and the environment.[16,17] However, recent experiments have challenged a direct link between Auger recombination and blinking, since the dark quantum dot state does not necessarily exhibit the dramatic reduction in fluorescence lifetime indicative of increased nonradiative decay.[13] Clearly, surface traps can play a crucial role in quantum dot emission, which is readily visualized by considering the long-time luminescence decay dynamics.[18,19] Much like in the case of amorphous organic semiconductor films,[20] these transients in ensemble systems tend to follow power laws of the same exponent as the intermittency his-

tograms recorded for single particles,[21,22] suggesting a direct link between blinking and trap filling.

We recently demonstrated that the charge-separated state in semiconductor core-shell nanorod structures can be exploited to electrostatically store excitation energy for over 10^5 times the fluorescence lifetime by spatially isolating the electron and hole of the exciton.[23] The storage mechanism can be described as a reversible transition between a direct radiative and an indirect nonradiative exciton state.[24–28] This nonradiative state is more reminiscent of spatially charge-separated excitations in coupled quantum well structures than of dipole-forbidden excitations such as the dark exciton in CdSe or triplet excitons in molecular semiconductors.[29–31] Given the common assumption that charge separation should lead to charging of the quantum dot core, making it nonemissive by the Auger mechanism,[10] it is not clear how the proposed electrostatic formation and long-timescale storage of charge-separated excitons arise. Here, we describe a detailed study of exciton storage in CdSe/CdS tetrapod structures, with the aim of identifying the effects of the electric field on the excited state thermalization and the consequences for both the light-harvesting process from the tetrapod arms, as well as multiexciton formation and relaxation in the nanocrystal. Exciton storage is found to be due to discrete localized states (i.e., trap sites), which fill up with increasing excitation density. However, the external electric field is unable to store multiexciton states, thus suggesting that the electrical manipulation of the excited state carrier location within the nanostructures is not an instantaneous process and is slower than the relaxation time of multiexciton states. This control mechanism of carrier location and single exciton lifetime offers routes to designing building blocks for excitonic circuits and opens a direct spectroscopic window to surface trap states, which play a crucial role in the photophysics of these materials.
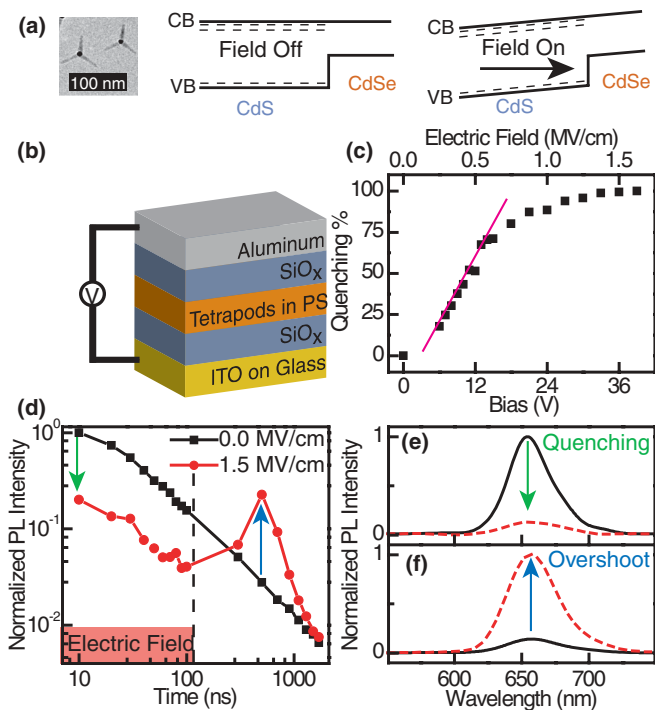
FIG. 1. (Color online) Separation and storage of excitons in an electric field. (a) Transmission electron micrograph and schematic of the electronic structure of CdSe/CdS core-shell tetrapods in and out of an external electric field, where the dashed lines represent localized states, while the solid lines depict the quantum-confined band states (CB, conduction band, VB, valence band). (b) Structure of the device enabling time-resolved electromodulation of the fluorescence. (c) The PL quenching efficiency as a function of applied external electric field (i.e., device bias) shows an initial linear dependence followed by saturation. The solid pink line serves as a guide to the eye, showing a linear dependence. (d) The time-resolved PL within the electric field shows substantial quenching but the same power-law decay dynamics, followed by an intensity overshoot upon removal of the external field. (e), (f) Corresponding emission spectra of quenching and overshoot (solid black: unmodulated; dashed red: modulated).

II. TETRAPOD NANOCRYSTALS AND FIELD-INDUCED LUMINESCENCE QUENCHING

A transmission-electron micrograph of the CdSe/CdS tetrapod nanocrystals used in this study is shown in Fig. 1(a) alongside a one-dimensional schematic depicting both the quantum confined band states and a distribution of traps states in a CdSe/CdS nanocrystal with and without an external electric field applied. The tetrapod structures are composed of a 4-nm-diameter CdSe core that is surrounded by a CdS shell consisting of four arms of ~30 nm in length. These particles are appealing for investigations of the effects of electric field manipulation. The bulky arms effectively prevent aggregation between cores, which cannot be fully excluded in the CdSe/CdS sphere-rod structures studied previously.[23] With the tetrapods, one can therefore be certain that electric field effects arise purely from the intraparticle electronic structure, and not from bulk-like interactions between particles. Secondly, the absorption cross section of the CdS arms in the ultraviolet (UV) spectrum, where optical excitation occurs, is over 300 × larger

than that of CdSe.[32] Efficient relaxation of excitons generated in the arms to the core therefore enables the generation of very high excitation densities within the cores,[33–35] leading to the formation of emissive multiexciton states.[35–39] In addition, the greater level of symmetry of the tetrapods compared to nanorods suggests that separating electron and hole of the exciton should be more facile in the former than in the latter: Only nanorods with preferential orientation in the electric field will allow exciton storage, whereas for the tetrapods, all electric field orientations should lead to carrier separation.

We studied the nanosecond to microsecond photoluminescence (PL) dynamics of the tetrapod nanocrystals with and without an external electric field applied. Figure 1(b) displays the basic capacitive device geometry employed, as described previously,[23] consisting of two electrodes with insulating layers to prevent charge injection, and a spin-coated dispersion of the nanocrystals in polystyrene. We note that great care has to be taken when choosing deposition rates and the overall thickness to prevent the formation of pinholes, which can lead to current breakdown of the device. In addition, the high pulse energies of the exciting laser necessitate the use of very thin (200 μm) glass substrates to minimize background emission from the glass. All of the measurements involving prompt luminescence from the device structures were conducted in vacuum at room temperature. Experiments involving the much weaker delayed luminescence monitored by time-gated detection were performed at 25 K, where the deleterious background emission from the polystyrene matrix and the glass substrate is minimized. The luminescence of the device was excited by a pulsed solid state laser operating at 355 nm with a 700 ps pulse length and variable (typically 200 Hz) repetition rate and pulse energy (up to 100 μJ). Electric fields were applied to the device by a pulsed voltage source (Agilent 8114A pulse generator), and the emission was dispersed with a spectrometer and recorded with a gated intensified charge-coupled device (ICCD) camera (Andor iStar). Figure 1(c) shows the relative change in emission intensity, or quenching efficiency, as a function of electric field. The quenching efficiency is defined as the field-induced reduction in PL emission normalized to the unperturbed emission intensity ($\Delta I/I = 1 - I_{E \neq 0}/I_{E=0}$). For low fields, the fluorescence quenching appears to follow a linear relationship, in contrast to the parabolic dependence reported for CdS nanocrystals.[40] This different functional dependence on field strength may arise from both the intrinsically different electronic structure of the heterostructure, as well as the different geometry of the tetrapod. Above 0.5 MV/cm, the quenching efficiency begins to saturate and reaches a maximum of 95%. Thus, at most, only one in twenty tetrapods are not affected by the external electric field, suggesting that suitable carrier separation and electrostatic control of photoluminescence are possible in nearly all of the individual nanocrystals. The quenched PL can be recovered in part by removal of the electric field in a pulsed experiment, which can be seen in Fig. 1(d), where the luminescence decay is plotted on a double-logarithmic representation following a laser pulse at time zero. The black curve shows the emission decay at zero field, which follows the expected power-law dependence.[18] Under application of an electric-field pulse up to time 100 ns, the power-law dependence is unperturbed, but the delayed recombination
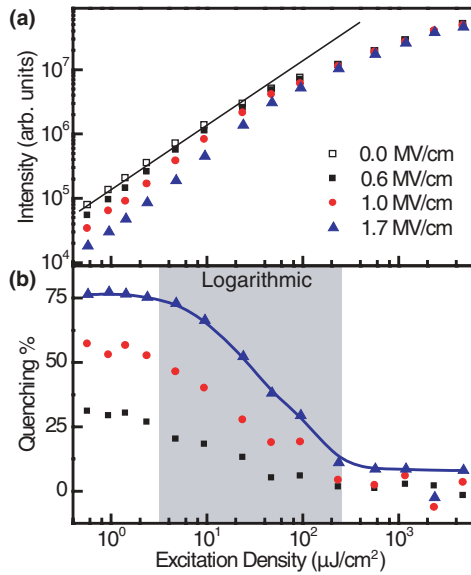
FIG. 2. (Color online) Dependence of prompt PL intensity and quenching efficiency on excitation density at different external electric field strengths. (a) PL intensity dependence of the tetrapods on excitation density in the presence of different external fields, where the black line depicts a linear relationship. (b) The PL quenching efficiency of the same device in corresponding external electric fields shows a logarithmic decrease with increasing excitation density to a uniform saturation point. The blue (solid) line is a guide to the eye.

is quenched by almost an order of magnitude. Removal of the field at time 100 ns leads to a recombination burst as separated charge-carrier pairs stabilized in the external field can now recombine: Excitons can be stored electrostatically in the tetrapods. The corresponding emission spectra under quenching and overshooting conditions are shown in Fig. 1(e) and 1(f), respectively, and do not exhibit any dramatic difference to the unperturbed emission spectra, demonstrating that emission in all cases arises from the same quantum-confined CdSe excitonic species.

III. CHARACTERIZATION AND DISCUSSION OF FIELD-INDUCED QUENCHING BEHAVIOR

A. Dependence of quenching on excitation density

To gain better insight into the electronic states involved in the exciton storage process, we probe the effect of excitation density on the quenching efficiency of the CdSe core emission as shown in Fig. 2. We find a strong dependence of the electrical fluorescence quenching efficiency on the excitation density per laser pulse. Figure 2(a) shows the PL intensity as a function of excitation density under different external field strengths. For all external fields, the PL intensity follows the expected linear dependence on excitation density over two orders of magnitude. Above 10 μJ/cm^2, the dependence assumes a sublinear functionality, which arises from the formation of multiexcitonic states and the associated increase in nonradiative Auger recombination.[37,38,41,42] Figure 2(b) plots the quenching efficiency in the 2 ns window following the laser pulse as a function of excitation density for three

different field strengths. While the field strength affects the initial, maximum quenching amplitude, all three curves show the same functional dependence. Small excitation densities below 2 μJ/cm^2 have a negligible effect on the quenching efficiency. Above this excitation density, however, the quenching efficiency of the device logarithmically approaches a minimum of almost 0% over nearly two orders of magnitude in excitation density. Even though the PL intensity still increases with excitation density [Fig. 2(a)], the quenching efficiency saturates at this minimum value. Furthermore, the saturation point of ~200 μJ/cm^2 is ubiquitous for all three of the external field strengths, suggesting that it is an intrinsic property of the tetrapod ensemble and that significant quenching of the exciton can no longer occur, regardless of the electric field strength. Since the excitation density at which the relative quenching saturates is independent of the external field strength, and because no significant dependence of the quenching functionality on either laser repetition rate (from 1 to 200 Hz) or temperature (from room temperature to 25 K) is observed, we exclude the possibility that saturation of the quenching is due to electrostatic screening from the formation of a persistent space charge in the surrounding matrix. Furthermore, while only one representative device is shown here, such a logarithmic dependence of the quenching efficiency on excitation density was seen in all of the devices tested. We therefore conclude that the quenching efficiency for tetrapod CdSe/CdS nanocrystals is dependent on the excited state carrier population, and propose that each nanocrystal has a distinct threshold in the population of excited state carriers above which additional excitations can no longer be quenched. At present, the precise origin of the logarithmic dependence of quenching on excitation density is not fully clear, although one may speculate that it could be indicative of a diffusive process, i.e., due to diffusion of excitons to quenching centers.

B. The role of localized trap states

By delaying the electric field pulse with respect to the optical excitation, we are able to differentiate the contributions to the exciton storage effect of delocalized band states from those of localized trap states. Accordingly, we reverse the experiment and apply an electric field pulse following the laser pulse at times exceeding the exciton lifetime, thus specifically probing any long-lived trapped charges. In this way, we can drive trapped charges, which are created due to spontaneous ionization of the exciton, to recombine,[3,6,14,43] assuming that they have preferential orientation with respect to the electric field. Figure 3(a) plots the transient PL intensity for a device with and without an electric field pulse applied between times 1000 ns and 1800 ns after laser excitation. The transient luminescence decay follows the common power-law dependence. At the onset of the electric field pulse, the luminescence rises by a factor of three, only to be quenched subsequently by an order of magnitude. After removal of the electric field, the usual overshoot occurs. The overshoot at the *onset* of the pulse can only result from detrapping of charges in the nanocrystal, which is then followed by formation and recombination of core excitons. The onset and decay of the overshoot signals are primarily limited by the speed at which the electric field can be applied, i.e., by the RC
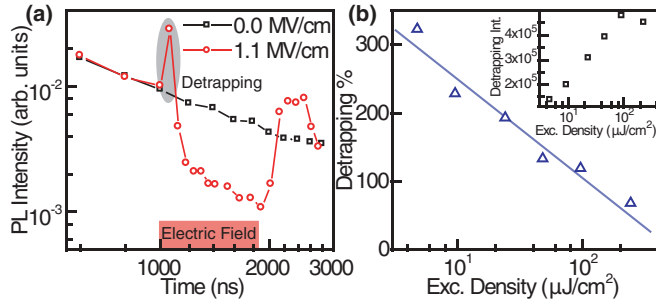
FIG. 3. (Color online) Transient luminescence of a device for which the electrical pulse is applied after excitation by a laser pulse. (a) The recombination rate of intrinsically generated trapped excitations is initially increased by the electric field pulse, which promotes charge detrapping of carrier pairs with dipoles parallel to the electric field. Each data point corresponds to an integral measurement using the gated ICCD camera for a particular gate width at a certain delay time after the exciting laser pulse. (b) The relative intensity of the electrically induced PL burst decreases with increasing excitation density due to the limited population of trap states in the individual nanoparticle. The inset in (b) shows the absolute area of the PL burst, which grows logarithmically with excitation density until it appears to saturate at large excitation densities. The PL burst was measured in a 60 ns integration window, delayed 1040 ns after the laser trigger.

time of the device, which is typically between 250 ns and 500 ns. Figure 3(b) plots the relative area of the detrapping peak, measured by integrating the emission between 1040 ns and 1100 ns after the laser pulse. This integrated overshoot intensity decreases logarithmically with excitation density in a similar fashion to the quenching of the luminescence [Fig. 2(b)]. Further, the absolute area of the detrapping peak shows a logarithmic *growth*, which appears to also saturate at large excitation density as shown in the inset of Fig. 3(b). The remarkably similar dependence of the detrapping overshoot peak on excitation density to that of the PL quenching strongly suggests that the observed exciton storage effect is mediated through long-lived localized states of the nanocrystal.

Consideration of the dynamics presented here for tetrapods in addition to our past work on nanorods,[8,23] leads us to propose that the primary states responsible for the formation of these charge-separated excitons in the presence of an external electric field are the localized trap states,[3,6,43–45] as opposed to the quantum-confined band states of the nanocrystal. The conduction and valence band offsets of CdSe and CdS are such that, to a first approximation, a quasi type-II heterostructure is formed [Fig. 1(a)],[46] where the excited electron state spans the two materials while the hole state is confined in the lower-gap CdSe. Intuitively, one would therefore expect an external electric field to simply shift the center of the electron wave function out of the CdSe and into the CdS, thus reducing overlap with the hole and lowering the radiative rate and emission strength. One would also expect such an effect to depend on the excited state carrier population due to increasing Coulombic repulsion with increasing population.[35,38,39] However, careful consideration of the reduced overlap of the delocalized states in the presence of an electric field for nanorods of similar aspect ratio shows that this effect alone is unlikely to account for

exciton storage on timescales orders of magnitude longer than the unperturbed exciton lifetime.[8,23] Rather, the timescales presented here and in the nanorod work strongly suggest that localized defect or trap states with small oscillator strengths and long lifetimes are a crucial ingredient in the exciton storage effect reported for these CdSe/CdS systems.

It is known that such localized states, or traps, can be present on the surface of CdS.[47] For example, a signature of these localized states is the increase of direct CdS exciton recombination in tetrapods of increasing arm length.[42] In addition, it has been suggested that an interfacial barrier can be formed in the conduction band between the CdSe and the CdS due to the strain arising from the lattice mismatch and the associated internal electric field.[46] Such traps are apparently crucial for enabling long-timescale electrical exciton storage through the electrostatic separation of the excited state carriers. This situation is equivalent to the case of exciton storage in coupled quantum wells.[25,26,48] Furthermore, virtually all of the tetrapods must have such trap sites since, at low excitation density, the relative fluorescence quenching tends towards 100% [Fig. 1(c)]. Once all of the suitable CdS trap sites are filled within an individual nanocrystal, any further excitons generated during the excitation pulse can no longer be stored; the CdSe core radiates unperturbed as it would in the absence of an external field, as seen by the saturation of quenching in Fig. 2(b). In addition to trap filling, increased Coulombic screening within the nanoparticle during the excitation pulse could play a role in the saturation of the quenching, but we suspect that it is secondary, since the estimated per-particle exciton population numbers[42] at these excitation levels constitute an insufficient carrier density to substantially screen the external field. In addition, it is hard to rationalize how accumulation of local charges in the vicinity of the nanoparticle would lead to *isotropic* screening of the external field, i.e., effective suppression of quenching for all particle orientations. Strikingly, the observed saturation of the quenching also indicates that the separated carriers do not increase the nonradiative recombination pathways such as Auger recombination. Thus, it appears that neither the external electric field nor the separated carriers greatly affect the primary exciton states with short lifetimes.

C. External field effects on multiexciton states

To further probe the quenching and storage process on primary excitons, we address the question of the influence of the electric field on multiexciton states and the underlying relaxation mechanism from the arm to the core. Under conditions of sufficiently strong pumping, emission in addition to the regular CdSe exciton can result from CdS rod excitons[42] or from CdSe core multiexcitons.[36–39] Due to the competition with nonradiative Auger processes, multiexciton states typically decay within a few hundred picoseconds.[35,38,39,41,49] Figure 4 summarizes the electromodulated luminescence spectroscopy of the tetrapods at high excitation density. Multiple excitons can be generated either at once within one arm, or in multiple arms of the tetrapod, as sketched in Fig. 4(a). Emission may then either occur directly from the arm (labeled X_A), or from the core as a regular exciton (X) or a multiexciton state, such as the biexciton (X_B) or the triexciton (X_T).[36,38,49] The
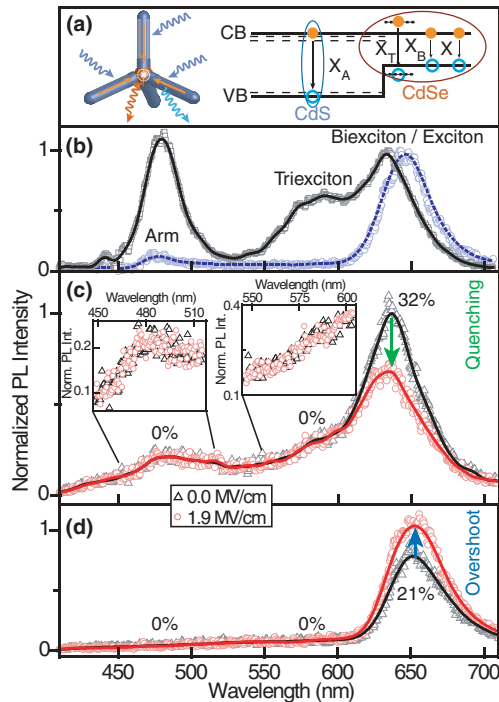
FIG. 4. (Color online) Multiexciton emission from tetrapods at high excitation densities. (a) Simultaneous absorption of multiple photons in an individual nanoparticle can lead to emission either from the arm (X_A), the core (X), or multiexciton states in the core such as the biexciton (X_B) and triexciton (X_T). (b) Comparison of gated picosecond luminescence spectra of a solution of nanocrystals in toluene (excitation with a 140 fs laser pulse, detection in a 0–40 ps time window) at high (solid black curve) and low (dashed blue curve) excitation densities clearly reveals the spectral signatures of the multiexciton states. (c) Electric field quenching in devices is only observed in the core exciton channel, not for the arm exciton, biexciton, or triexciton. (d) Consequently, the stored excitation energy after removal of the electric field pulse returns solely as single exciton core emission.

four intraparticle species are clearly observed in time-resolved fluorescence spectra. Due to the fast decay of the multiexcitons, we employed a combination of femtosecond laser excitation with picosecond streak camera detection to clearly resolve the different features. Using pulsed excitation at 400 nm (pulse length 140 fs, repetition rate 80 MHz), Fig. 4(b) illustrates the spectral signatures of the multiexciton states by comparing the PL spectrum of a solution of tetrapods in toluene in a 40 ps time window after excitation at high excitation density (9 μJ/cm^2) to the spectrum at low excitation density (0.2 μJ/cm^2). The PL spectrum at high excitation density shows three notable differences to that at low excitation density: (1) The main luminescence peak shifts ∼10 meV to higher energies, which is attributed to the Coulombic repulsion present in the biexciton;[38,39] (2) a luminescence peak appears at ∼580 nm, which is assigned to the triexciton state;[37,38] and (3) a luminescence peak at ∼480 nm arises due to radiative recombination in the CdS arms.[42] The three visible peaks display the characteristic power dependence: linear for the arm emission, linear to sublinear for the core exciton, and quadratic for the core triexciton (data not shown), in agreement with the

results published by Sitt *et al.*[38] The small protrusion at 445 nm arises due to Raman scattering from the solvent.

The same spectral features are visible in the nanosecond PL spectra of the thin-film devices, albeit with reduced amplitudes of the multiexcitons due to the longer optical gate length of 2 ns in detection using the intensified camera rather than the streak system. To test for the influence of the electric field, we chose the lowest excitation density for which triexciton emission could be clearly resolved, and sufficiently high electric field pulses to ensure substantial quenching. As Fig. 4(c) reveals, application of the field only reduces the intensity of the main luminescence peak. All of the signatures of the multiexciton states (the CdS arm emission, the triexciton emission, and the spectral shift of the main peak due to the biexciton) remain. In contrast, upon removal of the electric field, the spectrum of the fluorescence overshoot [Fig. 4(d)] loses all signatures of the multiexciton states and returns to the form seen under low excitation density. We therefore conclude that neither the arm exciton nor the core multiexciton states, which all have lifetimes less than a few hundred picoseconds, can be quenched or stored electrically. This observation further indicates that the quenching induced by carrier separation requires trapping of the excited carriers in localized states on timescales that exceed those of ultrafast carrier thermalization and multiexciton recombination.[33,35] Consequently, exciton storage at these field strengths is not an instantaneous electrostatic effect, in contrast to, for example, the quantum-confined Stark effect.[50] Rather, the external field promotes the ultimate localization of carriers to long-lived nonradiative states without drastically changing the ultrafast thermalization dynamics. We note that larger external fields, which are inaccessible to our device structure due to dielectric breakdown, may be able to separate and store these band excited states with short radiative lifetimes, leading to exciton storage that is indeed an *instantaneous* electrostatic effect, as opposed to what is shown here.

IV. CONCLUSION AND SUMMARY

We have demonstrated that the quenching and storage of excitons in CdSe/CdS nanocrystals arise from the presence of nanocrystal trap states, which can be reversibly filled and emptied by the application of an electric field. Formation of such a charge-separated state within the particle does not necessarily render it nonemissive, or else the saturation of electric field quenching at high excitation densities would not be discernible. In the context of unraveling the underlying mechanisms of quantum dot blinking, it is therefore crucial to develop a deeper understanding of metastable charge-separated states within the single particle, which can reversibly feed the core exciton and can constitute a dominant mechanism for the recombination dynamics.

*Corresponding author: john.lupton@physik.uni-regensburg.de

[1] D. V. Talapin, J. S. Lee, M. V. Kovalenko, and E. V. Shevchenko, Chem. Rev. **110**, 389 (2010).

[2] M. Shim and P. Guyot-Sionnest, J. Chem. Phys. **111**, 6955 (1999).

[3] T. D. Krauss and L. E. Brus, Phys. Rev. Lett. **83**, 4840 (1999).

[4] R. Krishnan, M. A. Hahn, Z. H. Yu, J. Silcox, P. M. Fauchet, and T. D. Krauss, Phys. Rev. Lett. **92**, 216803 (2004).

[5] J. Müller, J. M. Lupton, A. L. Rogach, J. Feldmann, D. V. Talapin, and H. Weller, Phys. Rev. B **72**, 205339 (2005).

[6] E. Rothenberg, M. Kazes, E. Shaviv, and U. Banin, Nano Lett. **5**, 1581 (2005).

[7] S. A. Empedocles and M. G. Bawendi, Science **278**, 2114 (1997).

[8] J. Müller, J. M. Lupton, P. G. Lagoudakis, F. Schindler, R. Koeppe, A. L. Rogach, J. Feldmann, D. V. Talapin, and H. Weller, Nano Lett. **5**, 2044 (2005).

[9] L. Jdira, K. Overgaag, J. Gerritsen, D. Vanmaekelbergh, P. Liljeroth, and S. Speller, Nano Lett. **8**, 4014 (2008).

[10] A. L. Efros and M. Rosen, Phys. Rev. Lett. **78**, 1110 (1997).

[11] S. J. Park, S. Link, W. L. Miller, A. Gesquiere, and P. F. Barbara, Chem. Phys. **341**, 169 (2007).

[12] J. Zhao, G. Nair, B. R. Fisher, and M. G. Bawendi, Phys. Rev. Lett. **104**, 157403 (2010).

[13] C. Galland, Y. Ghosh, A. Steinbrück, M. Sykora, J. A. Hollingsworth, V. I. Klimov, and H. Htoon, Nature **479**, 203 (2011).

[14] R. M. Kraus, P. G. Lagoudakis, J. Müller, A. L. Rogach, J. M. Lupton, J. Feldmann, D. V. Talapin, and H. Weller, J. Phys. Chem. B **109**, 18214 (2005).

[15] B. D. Gerardot, D. Brunner, P. A. Dalgarno, P. Öhberg, S. Seidl, M. Kroner, K. Karrai, N. G. Stoltz, P. M. Petroff, and R. J. Warburton, Nature **451**, 441 (2008).

[16] J. Antelman, Y. Ebenstein, T. Dertinger, X. Michalet, and S. Weiss, J. Phys. Chem. C **113**, 11541 (2009).

[17] X. Wang, X. Ren, K. Kahen, M. A. Hahn, M. Rajeswaran, S. Maccagnano-Zacher, J. Silcox, G. E. Cragg, A. L. Efros, and T. D. Krauss, Nature **459**, 686 (2009).

[18] P. H. Sher, J. M. Smith, P. A. Dalgarno, R. J. Warburton, X. Chen, P. J. Dobson, S. M. Daniels, N. L. Pickett, and P. O'Brien, Appl. Phys. Lett. **92**, 101111 (2008).

[19] M. Jones, S. S. Lo, and G. D. Scholes, Proc. Natl. Acad. Sci. USA **106**, 3011 (2009).

[20] A. Gerhard and H. Bassler, J. Chem. Phys. **117**, 7350 (2002).

[21] I. H. Chung and M. G. Bawendi, Phys. Rev. B **70**, 165304 (2004).

[22] J. Tang and R. A. Marcus, J. Chem. Phys. **123**, 204511 (2005).

[23] R. M. Kraus, P. G. Lagoudakis, A. L. Rogach, D. V. Talapin, H. Weller, J. M. Lupton, and J. Feldmann, Phys. Rev. Lett. **98**, 017401 (2007).

[24] C. Rocke, S. Zimmermann, A. Wixforth, J. P. Kotthaus, G. Böhm, and G. Weimann, Phys. Rev. Lett. **78**, 4099 (1997).

[25] T. Lundstrom, W. Schoenfeld, H. Lee, and P. M. Petroff, Science **286**, 2312 (1999).

[26] A. A. High, E. E. Novitskaya, L. V. Butov, M. Hanson, and A. C. Gossard, Science **321**, 229 (2008).

[27] H. J. Krenner, C. E. Pryor, J. He, and P. M. Petroff, Nano Lett. **8**, 1750 (2008).

[28] C. L. Choi, H. Li, A. C. K. Olson, P. K. Jain, S. Sivasankar, and A. P. Alivisatos, Nano Lett. **11**, 2358 (2011).

[29] M. Nirmal, D. J. Norris, M. Kuno, M. G. Bawendi, A. L. Efros, and M. Rosen, Phys. Rev. Lett. **75**, 3728 (1995).

[30] O. Labeau, P. Tamarat, and B. Lounis, Phys. Rev. Lett. **90**, 257404 (2003).

[31] M. Reufer, M. J. Walter, P. G. Lagoudakis, A. B. Hummel, J. S. Kolb, H. G. Roskos, U. Scherf, and J. M. Lupton, Nat. Mater. **4**, 340 (2005).

[32] D. V. Talapin, J. H. Nelson, E. V. Shevchenko, S. Aloni, B. Sadtler, and A. P. Alivisatos, Nano Lett. **7**, 2951 (2007).

[33] M. G. Lupo, D. F. Sala, L. Carbone, M. Zavelani-Rossi, A. Fiore, L. Lüer, D. Polli, R. Cingolani, L. Manna, and G. Lanzani, Nano Lett. **8**, 4582 (2008).

[34] C. Mauser, E. Da Como, J. Baldauf, A. L. Rogach, J. Huang, D. V. Talapin, and J. Feldmann, Phys. Rev. B **82**, 081306 (2010).

[35] M. Zavelani-Rossi, M. G. Lupo, F. Tassone, L. Manna, and G. Lanzani, Nano Lett. **10**, 3142 (2010).

[36] B. Fisher, J. M. Caruge, D. Zehnder, and M. Bawendi, Phys. Rev. Lett. **94**, 087403 (2005).

[37] V. I. Klimov, Annu. Rev. Phys. Chem. **58**, 635 (2007).

[38] A. Sitt, D. F. Sala, G. Menagen, and U. Banin, Nano Lett. **9**, 3470 (2009).

[39] M. Saba, S. Minniberger, F. Quochi, J. Roither, M. Marceddu, A. Gocalinska, M. V. Kovalenko, D. V. Talapin, W. Heiss, A. Mura, and G. Bongiovanni, Adv. Mater. **21**, 4942 (2009).

[40] M. S. Mehata, M. Majumder, B. Mallik, and N. Ohta, J. Phys. Chem. C **114**, 15594 (2010).

[41] V. I. Klimov, A. A. Mikhailovsky, S. Xu, A. Malko, J. A. Hollingsworth, C. A. Leatherdale, H.-J. Eisler, and M. G. Bawendi, Science **290**, 314 (2000).

[42] A. A. Lutich, C. Mauser, E. Da Como, J. Huang, A. Vaneski, D. V. Talapin, A. L. Rogach, and J. Feldmann, Nano Lett. **10**, 4646 (2010).

[43] J. A. Fairfield, T. Dadosh, and M. Drndic, Appl. Phys. Lett. **97**, 143112 (2010).

[44] J. J. Finley, M. Skalitz, M. Arzberger, A. Zrenner, G. Böhm, and G. Abstreiter, Appl. Phys. Lett. **73**, 2618 (1998).

[45] R. Beaulac, P. I. Archer, J. van Rijssel, A. Meijerink, and D. R. Gamelin, Nano Lett. **8**, 2949 (2008).

[46] N. J. Borys, M. J. Walter, J. Huang, D. V. Talapin, and J. M. Lupton, Science **330**, 1371 (2010).

[47] F. Zezza, R. Comparelli, M. Striccoli, M. L. Curri, R. Tommasi, A. Agostiano, and M. Della Monica, Synth. Met. **139**, 597 (2003).

[48] A. G. Winbow, A. T. Hammack, L. V. Butov, and A. C. Gossard, Nano Lett. **7**, 1349 (2007).

[49] D. Oron, M. Kazes, I. Shweky, and U. Banin, Phys. Rev. B **74**, 115333 (2006).

[50] M. E. Reimer, M. P. van Kouwen, A. W. Hidma, M. H. M. van Weert, E. P. A. M. Bakkers, L. P. Kouwenhoven, and V. Zwiller, Nano Lett. **11**, 645 (2011).